

CHEMISTRY

AN ASIAN JOURNAL

www.chemasianj.org

Accepted Article

Title: Conjugated Oligothiophene Derivatives Based on Bithiophene with Unsaturated Bonds as Building Block for Solution-Processed Bulk Heterojunction Organic Solar Cells

Authors: Chaohua Cui, Yue Wu, Man-Sing Cheung, Cheuk-Lam Ho, Qingchen Dong, Zhenyang Lin, Yongfang Li, and Wai Yeung Wong

This manuscript has been accepted after peer review and appears as an Accepted Article online prior to editing, proofing, and formal publication of the final Version of Record (VoR). This work is currently citable by using the Digital Object Identifier (DOI) given below. The VoR will be published online in Early View as soon as possible and may be different to this Accepted Article as a result of editing. Readers should obtain the VoR from the journal website shown below when it is published to ensure accuracy of information. The authors are responsible for the content of this Accepted Article.

To be cited as: *Chem. Asian J.* 10.1002/asia.201601281

Link to VoR: <http://dx.doi.org/10.1002/asia.201601281>

A Journal of



A sister journal of *Angewandte Chemie* and *Chemistry – A European Journal*

WILEY-VCH

Chem. Asian J.

Conjugated Oligothiophene Derivatives Based on Bithiophene with Unsaturated Bonds as Building Block for Solution-Processed Bulk Heterojunction Organic Solar Cells

Chaohua Cui,^{*[a, b]} Yue Wu,^[b] Man-Sing Cheung,^[c] Cheuk-Lam Ho,^[a] Qingchen Dong,^[d] Zhenyang Lin,^[c] Yongfang Li^[b] and Wai-Yeung Wong^{*[a, e]}

[a] Institute of Molecular Functional Materials, Department of Chemistry and Institute of Advanced Materials, Hong Kong Baptist University, Waterloo Road, Kowloon Tong, Hong Kong, P.R.China. E-mail: rwywong@hkbu.edu.hk

[b] Laboratory of Advanced Optoelectronic Materials, College of Chemistry, Chemical Engineering and Materials Science, Soochow University, Suzhou 215123, P.R. China. E-mail: cuichaohua@suda.edu.cn

[c] Department of Chemistry, The Hong Kong University of Science and Technology, Clearwater Bay, Kowloon, Hong Kong, P.R. China.

[d] MOE Key Laboratory for Interface Science and Engineering in Advanced Materials and Research Center of Advanced Materials Science and Technology, Taiyuan University of Technology, 79 Yingze West Street, Taiyuan 030024, P.R. China.

[e] Department of Applied Biology and Chemical Technology, The Hong Kong

Polytechnic University, Hung Hom, Hong Kong, P.R. China. E-mail:

wai-yeung.wong@polyu.edu.hk

Accepted Manuscript

Abstract

A new building block ATVTA which uses stiff carbon-carbon triple bonds (A) on 1,2-di(2-thienyl)-ethene (TVT) is developed. For comparing the effect of the three building blocks, the oligothiophene derivatives **S-01** with TVT unit, **S-02** with 5,5'-diethynyl-2,2'-dithienyl (AT2) unit and **S-03** with ATVTA were synthesized. Due to the better π -conjugation extension of TVT unit, **S-01** exhibits the most red-shifted absorption profile among them and **S-02** possesses the deepest HOMO level. While the HOMO level of **S-03** is down-shifted by 0.02 eV relative to that of **S-01**, the alkyne linkages can effectively down-shift the HOMO level. By replacing the terminal units of **S-03** with the stronger electron acceptors, **S-04** and **S-05** were prepared which exhibited broader absorption profiles and lower HOMO levels than that of **S-03**. Organic solar cells based on these molecules were fabricated and **S-03**:PC₆₀BM (1:1, w/w) based device afforded the highest V_{oc} value of 0.96 V and a PCE of 2.19%.

Keywords: Alkyne; Ethene; Oligothiophene; Organic solar cell; Synthesis

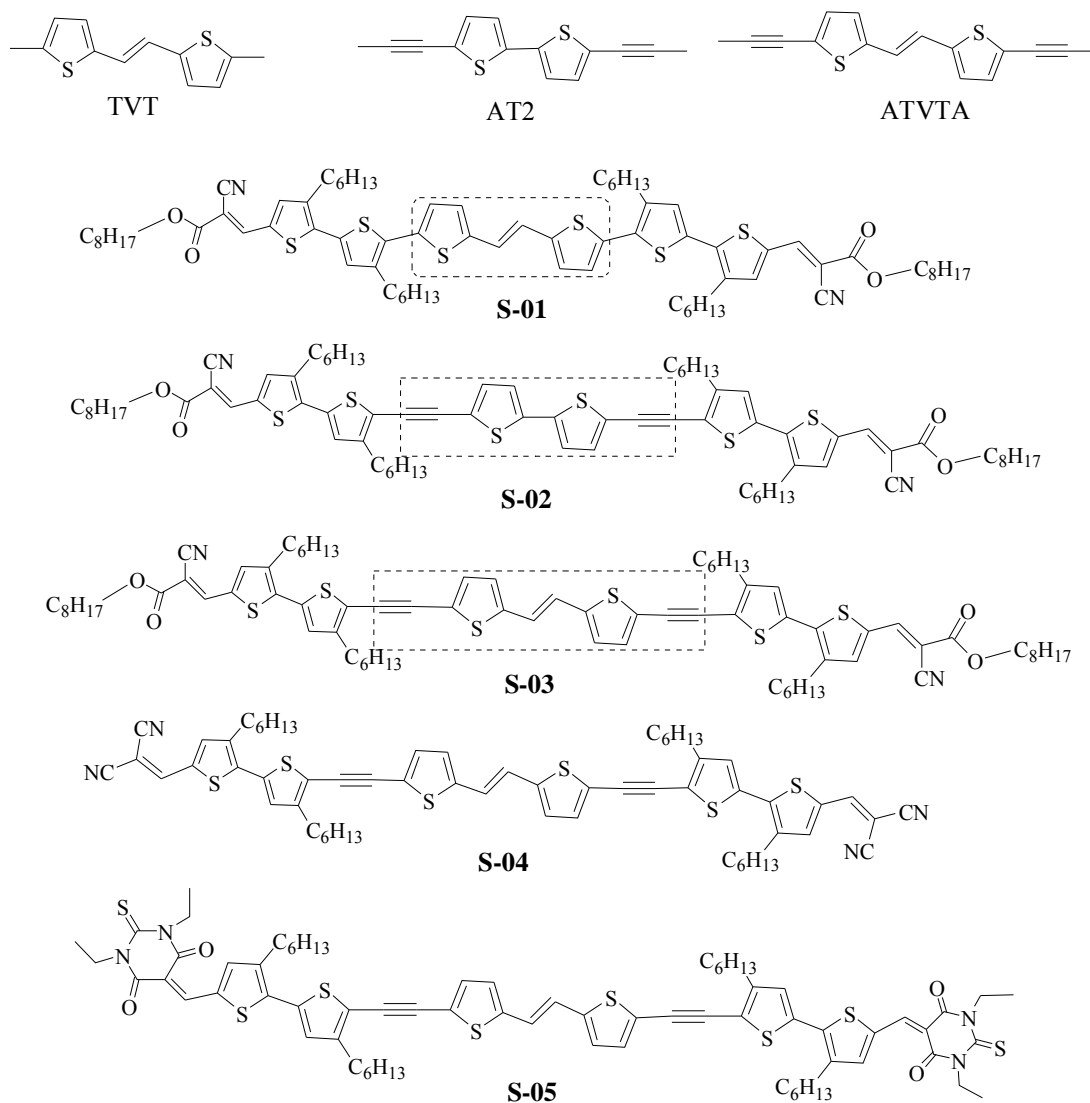
Introduction

Compared with solar cells based on inorganic materials, organic solar cells (OSCs) have attracted significant attention due to their attractive features, such as low-cost, light weight, easy fabrication and high mechanical flexibility.^[1-4] Bulk heterojunction (BHJ) solar cells are composed of a photoactive blend layer of electron-rich donor and electron-deficient acceptor sandwiched between an indium-tin oxide (ITO) positive electrode and a low work function metal negative electrode.^[5] Nowadays, high power conversion efficiency (PCE) is still the main concern of the studies on the OSCs. Materials innovation is one of the most effective approaches currently that can drive the performance of OSCs.^[6-17] The key issues of donor materials design include engineering the energy levels and bandgap to achieve high open-circuit voltage (V_{oc}) and short-circuit current density (J_{sc}), hence enhancing planarity to obtain high carrier mobility.^[18, 19]

It is well known that the π -conjugated backbone is the most important component in determining most of the OSC-related physicochemical properties of the conjugated donors. Thiophenes are considered as promising π -conjugated building blocks for extending π -conjugated backbone due to their remarkable electronic and redox properties as well as the prominent supramolecular behavior on the solid surface or in the bulk.^[20] In addition, thiophenes can be selectively modified by incorporation of the thiophene units into oligomers which render an effective conjugation along the main chain.^[21-23] Oligothiophenes possess extensive π -electron delocalization along the molecular backbone with well-known excellent charge transporting properties,

high polarizability, and tunable optical and electrochemical properties.^[24-26] Dipolar push-pull chromophores with highly polarizable π -electron systems involving a donor group and an acceptor group can serve as excellent donor materials in OSCs. They possess unique features such as the well-defined structures which make them synthetically reproducible, widen the light absorbing region to cover the low-energy spectrum, and favor the self-organization of the oligomers into ordered structures and close packing with increasing π - π orbital overlap due to the strong intermolecular interactions.^[27-29] Enlargement of the π systems is regarded as an efficient way to broaden the absorption spectra of donor materials to narrow their optical bandgaps, which is desirable for enhancing the J_{sc} value.^[30-33] For example, the essential structural feature of polymeric semiconductors in OSC applications is a π -conjugated backbone composed of linked unsaturated units, resulting in extended π orbitals along the polymer chain, and thus enabling proper charge transport and optical absorption.^[23, 34-36] 1,2-Di-(2-thienyl)-ethene (TVT) is a promising building block to extend π orbitals of the semiconducting materials.^[23, 37] Nevertheless, due to its electron-rich property, the HOMO energy levels of the resulting donor materials would probably be pushed up at the same time by introducing the TVT unit into the backbone, which will decrease the V_{oc} value. Here, we develop a new building block ATVTA (Scheme 1) which uses stiff carbon-carbon triple bonds as the linkage on TVT unit to tackle this issue. Introducing alkyne unit as the linkage is more accommodating than the alkene because of its reduced steric and conformational constraints.^[38, 39] We employed ATVTA as a building block of oligothiophene to

synthesize **S-03** (Scheme 1). The corresponding oligothiophenes **S-01** with TVT unit and **S-02** with with 5,5'-diethynyl-2,2'-dithienyl (AT2) unit were also synthesized for comparing the effect of the three building blocks (i.e. TVT, AT2 and ATVTA). The three small molecules show excellent solution processability, thermal stability and broad and strong absorption bands in the visible and near-infrared regions. Due to the better π -conjugation extension of TVT unit, **S-01** exhibits the most red-shifted absorption profile among the three molecules (**S-01** to **S-03**), and **S-03** shows slightly red-shifted absorption spectrum relative to that of **S-02**. On the other hand, **S-02** possesses the deepest HOMO energy level among the three molecules. Since the HOMO energy level of **S-03** is down-shifted by 0.02 eV as compared to that of **S-01**, the alkyne linkages are shown to down-shift the HOMO energy level of the resulting molecule. Using the simple spin-coating fabrication process to fabricate BHJ OSCs, the **S-01** and **S-02** based devices exhibited similar V_{oc} of 0.85 and 0.86 V, respectively, while S-03 based device afforded a very high V_{oc} value of 0.96 V, leading to a PCE of 2.19%. We replaced the terminal unit of **S-03** by the strong electron-withdrawing groups in **S-04** and **S-05** in order to further examine the effect of ATVTA building block. **S-04** and **S-05** exhibited broader absorption profiles and lower HOMO energy levels than that of **S-03**, which can be attributed to the stronger terminal acceptor units of **S-04** and **S-05**. The OSC devices based on **S-04** and **S-05** also demonstrated high V_{oc} values of 0.98 and 0.99 V, respectively. The results indicate that ATVTA unit is a promising building block for extending π -conjugated backbone without pushing up the HOMO energy levels, which guarantee the high V_{oc} value.



Scheme 1 Structures of S-01, S-02, S-03, S-04 and S-05.

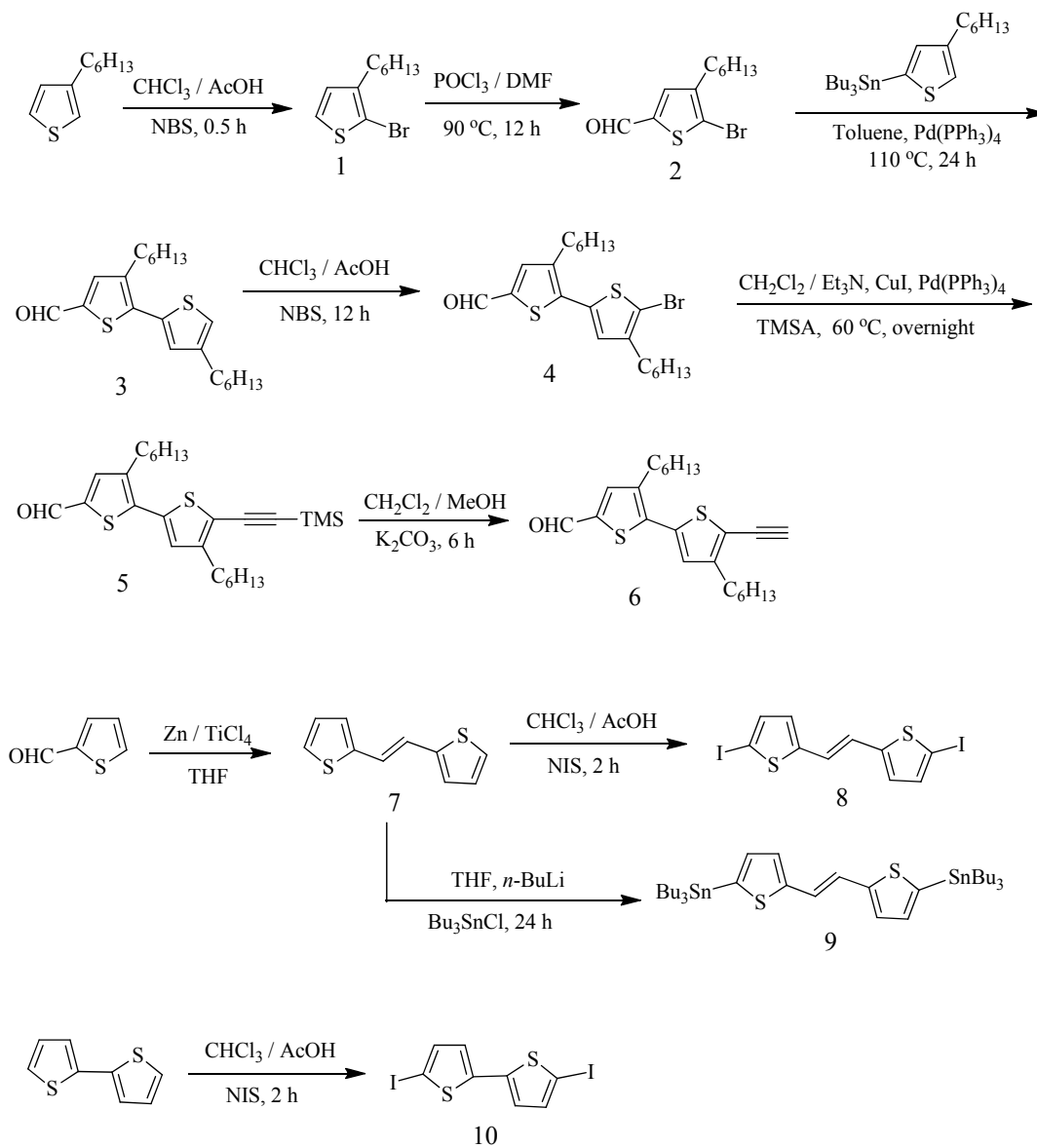
Results and Discussion

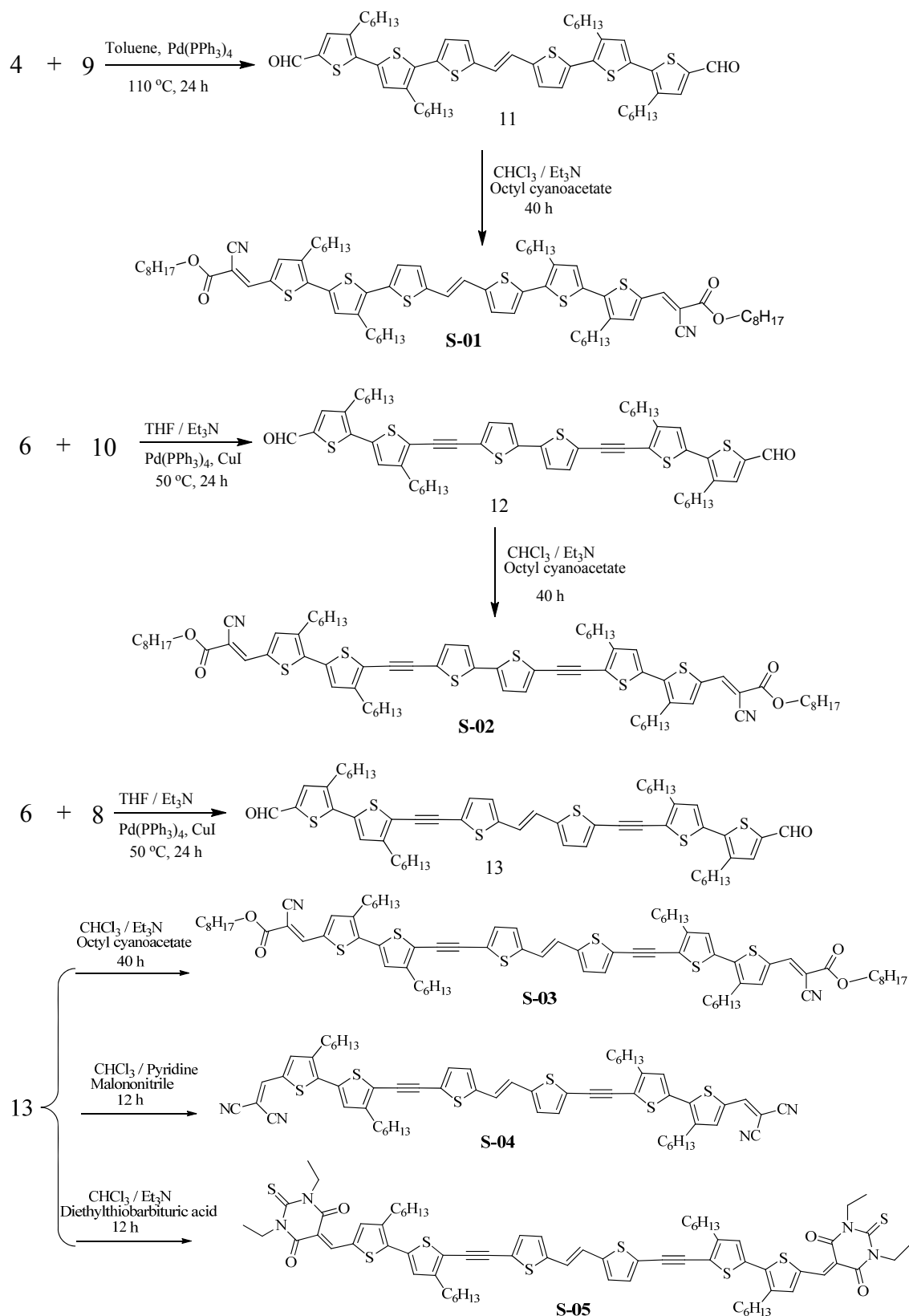
Syntheses and Characterization

The general synthetic routes towards all of the new compounds are outlined in Scheme 2. The key intermediate compound **4** was synthesized from Stille coupling between compound **2** and tributyl(4-hexylthiophen-2-yl)stannane, followed by bromination. This compound then underwent palladium-catalyzed Sonogashira

coupling reaction with trimethylsilylacetylene (TMSA) and the terminal alkyne was obtained by proto-desilylation approach using basic methanol solution to give the ethynyl precursor **6**. Bis-stannylated compound **9** was prepared in quantitative yield by forming dilithiated species followed by quenching with tributyltin chloride. The aldehydes **11**, **12** and **13** were then synthesized by Stille or Sonogashira coupling between compounds **4** and **9**, compounds **6** and **10**, as well as compounds **6** and **8**, respectively. The target molecules **S-01**, **S-02** and **S-03** were prepared by Knoevenagel condensation of aldehydes with octyl cyanoacetate in good yields. **S-04** and **S-05** were obtained by Knoevenagel condensation between an aldehyde-containing compound **13** and malononitrile and 1,3-diethyl-2-thiobarbituric acid, respectively.

All the small molecules exhibit excellent solubility in common organic solvents such as chloroform, toluene, dichloromethane and chlorobenzene. Their structures were unequivocally characterized by the techniques such as mass spectrometry, ^1H and ^{13}C NMR spectroscopy. The thermal stabilities of **S-01** to **S-05** were investigated by thermogravimetric analysis (TGA) and the temperatures with 5% weight-loss (T_d) are 355 °C, 327 °C, 322 °C, 405 °C and 373 °C, respectively. The stabilities of the three compounds are adequate for applications in OSCs and other optoelectronic devices. Figure 1 depicts the thermograms of **S-01** to **S-05**.





Scheme 2 Synthetic routes for **S-01**, **S-02**, **S-03**, **S-04** and **S-05**.

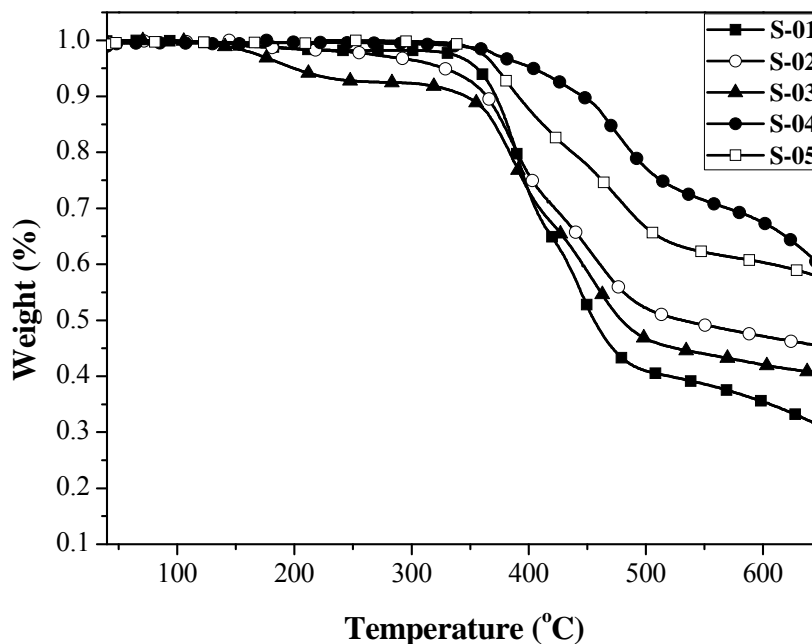
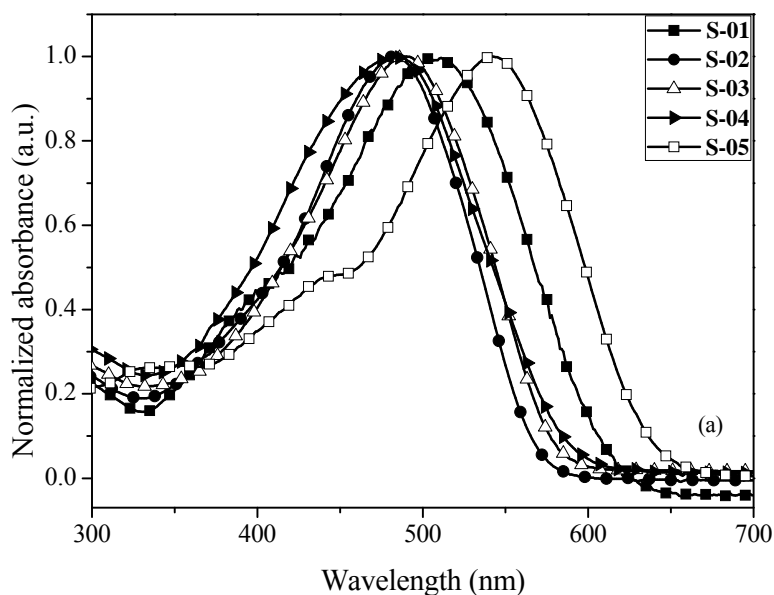


Figure 1 TGA plots of **S-01** to **S-05** with a heating rate of $20\text{ }^{\circ}\text{C min}^{-1}$ under nitrogen atmosphere.

Optical and Electrochemical Properties

Optical and redox properties of the compounds are important parameters for their application in OSCs. Figure 2 shows the ultraviolet-visible (UV-vis) absorption spectra of **S-01**, **S-02**, **S-03**, **S-04** and **S-05** in CH_2Cl_2 and in solid state. All of them exhibit strong absorption in the visible region, and the absorption coefficients of **S-01**, **S-02**, **S-03**, **S-04** and **S-05** are 1.1×10^5 , 8.0×10^4 , 6.3×10^4 , 5.9×10^4 and $4.6 \times 10^4\text{ M}^{-1}\text{ cm}^{-1}$, respectively. The well-defined absorption peaks with a vibronic shoulder in the long wavelength range (590-630 nm) of **S-01** to **S-03** imply the existence of ordered aggregation and strong π - π stacking. **S-01** film displays considerably broad and strong absorption profile with the absorption edge at 726 nm. By comparing **S-01** with **S-03**, the introduction of two carbon-carbon triple bonds into the system (**S-03**)

makes its absorption edge more blue-shifted (a blue-shift of 55 nm) than that of **S-01**. The absorption edge of **S-02** is also blue-shifted as compared with **S-01**. It appears that the carbon-carbon double bond acts as a better linker than the carbon-carbon triple-bond for conjugation extension to red-shift the absorption wavelength. Due to the strong electron accepting ability of the terminal units, **S-04** and **S-05** showed red-shifted absorption spectra than **S-03**, and **S-05** has the most red-shifted absorption band edge at *ca.* 723 nm with the corresponding band gap of 1.72 eV. The optical data of the compounds are summarized in Table 1 for a clear comparison.



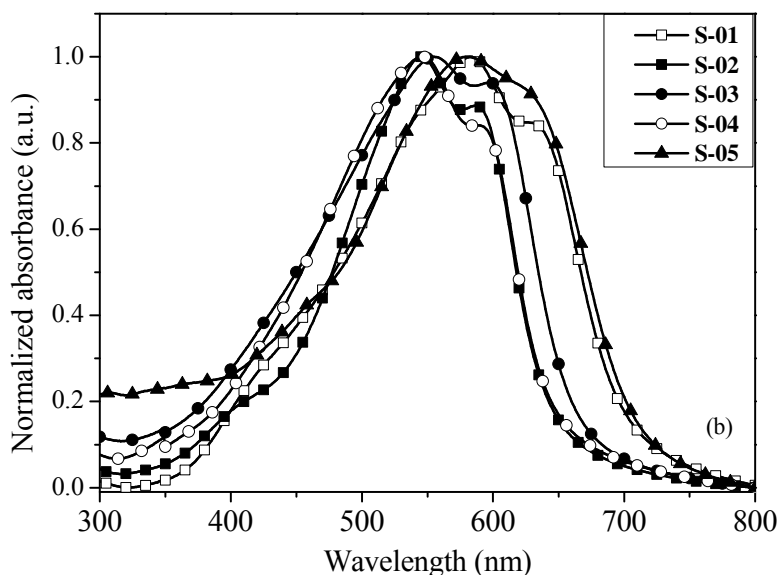


Figure 2 Absorption spectra of **S-01** to **S-05** in (a) CH_2Cl_2 and (b) thin film.

Figure 3 shows the cyclic voltammograms of **S-01**, **S-02**, **S-03**, **S-04** and **S-05** films on glassy carbon electrode in $0.1 \text{ mol L}^{-1} \text{ Bu}_4\text{NPF}_6$ acetonitrile solution. The onset reduction potentials (E_{red}) of **S-01**, **S-02** and **S-03** are -1.17 V , -1.23 V and -1.16 V vs. Ag/Ag^+ , and the onset oxidation potentials (E_{ox}) are 0.54 V , 0.64 V and 0.46 V vs. Ag/Ag^+ , respectively. Due to the stronger electron acceptance ability of their terminal groups, **S-04** and **S-05** show higher oxidation (0.67 and 0.68 V) potential than **S-03**. The HOMO and LUMO levels are calculated from the onset potentials of oxidation and reduction and by assuming the energy level of ferrocene/ferrocenium (Fc/Fc^+) to be -4.8 eV below the vacuum level.^[40] The formal potential of Fc/Fc^+ was measured as 0.07 V against Ag/Ag^+ . The HOMO and LUMO energy levels of **S-01** to **S-05** were calculated according to the following equations:

$$\text{HOMO} = -e(E_{\text{ox}} + 4.73) \text{ (eV)}$$

$$\text{LUMO} = -e(E_{\text{red}} + 4.73) \text{ (eV)}$$

where the units of E_{ox} and E_{red} are V vs. Ag/Ag^+ .

The HOMO energy levels of **S-01**, **S-02** and **S-03** are -5.27 , -5.37 and -5.29 eV, respectively. Among **S-01**, **S-02** and **S-03**, **S-02** shows the lowest HOMO energy level, while **S-03** shows a slightly lower HOMO energy level than **S-01**. Their calculated LUMO energy levels are -3.54 , -3.55 and -3.58 eV, respectively. The LUMO energy levels of **S-04** and **S-05** are -3.69 and -3.44 eV, and the HOMO energy levels are relatively low at -5.40 and -5.41 eV, respectively.

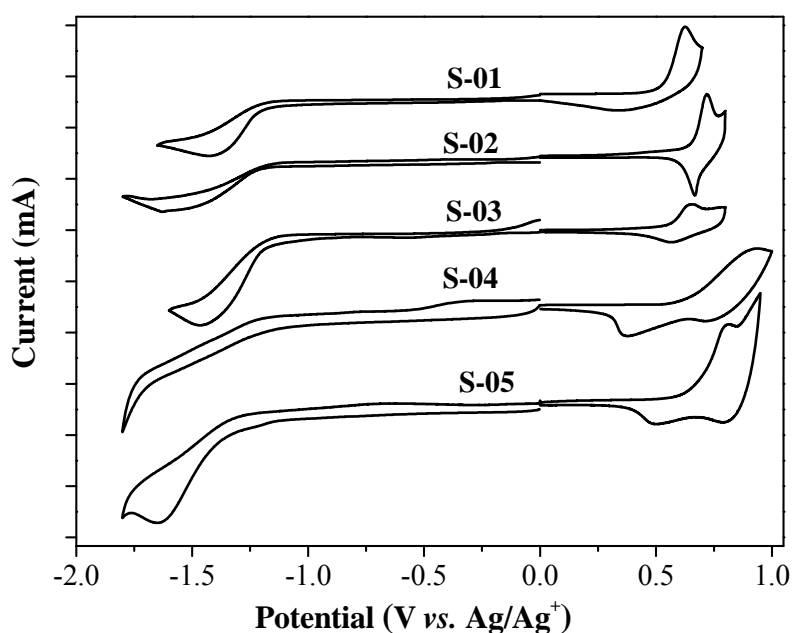


Figure 3 Cyclic voltammograms of the films for **S-01**, **S-02**, **S-03**, **S-04** and **S-05** on glassy carbon electrode in $0.1 \text{ mol L}^{-1} \text{ Bu}_4\text{NPF}_6$ acetonitrile solution at a scan rate of 100 mV s^{-1} .

Table 1 Optical and electrochemical properties of **S-01**, **S-02**, **S-03**, **S-04** and **S-05**.

	λ_{edge} [nm]	ϵ [$\text{M}^{-1} \text{ cm}^{-1}$]	E_g^{opt} [eV] ^a	HOMO [eV] ^b	LUMO [eV] ^b
S-01	726	1.1×10^5	1.71	-5.27	-3.56

S-02	682	8.0×10^4	1.82	-5.37	-3.55
S-03	671	6.3×10^4	1.85	-5.29	-3.57
S-04	679	5.9×10^4	1.83	-5.40	-3.69
S-05	723	4.6×10^4	1.72	-5.41	-3.44

^a E_g^{opt} , estimated from the optical absorption band edge of the thin film, $E_g^{\text{opt}} = 1240/\lambda_{\text{edge}}$. ^bHOMO = $-e(E_{\text{ox}} + 4.73)$ (eV); LUMO = $-e(E_{\text{red}} + 4.73)$ (eV).

Theoretical Calculations

To provide further insight into the fundamental aspects of molecular architecture, density functional theory (DFT) calculations for **S-01** to **S-05** were carried out. The molecular geometries, surface plots and HOMO and LUMO energy levels are displayed in Figure 4, and the results are shown in Table 2. It can be seen that although discrepancies exist between the calculation and experimental results, the trends of variation in the HOMO and LUMO energy levels are similar. From the results, the HOMO and LUMO are evenly distributed on the whole π -conjugated systems of the molecules.

The estimated bandgaps of **S-01**, **S-02** and **S-03** obtained from DFT calculations were found to be 2.04 eV, 2.19 eV and 2.09 eV, respectively. According to the calculation results, the introduction of carbon-carbon triple bonds as linkage increases the HOMO-LUMO gaps. In other words, carbon-carbon triple bond is not as a good linkage as the carbon-carbon double bond for extending π -conjugation. **S-04** and **S-05** show lower estimated bandgaps at 2.02 eV and 1.96 eV, respectively.

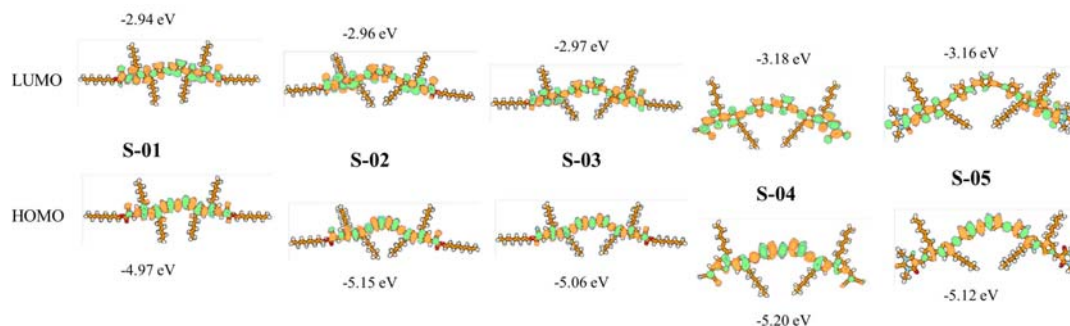


Figure 4 HOMO and LUMO energy levels and the frontier molecular orbitals obtained from DFT calculations on **S-01** to **S-05**.

Table 2 TDDFT calculation results of **S-01** to **S-05**.

Compound	The largest coefficient in the CI expansion of the T_1 state ^a ($S_0 \rightarrow T_1$ excitation energy)	The largest coefficient in the CI expansion of the S_1 state ^a ($S_0 \rightarrow S_1$ excitation energy)	The oscillator strength (f) of the $S_0 \rightarrow S_1$ transition
S-01	H→L: 0.71 (1133.0 nm)	H→L: 0.65 (681.1 nm)	2.8506
S-02	H→L: 0.66 (986.2 nm)	H→L: 0.66 (637.5 nm)	2.9374
S-03	H→L: 0.67 (1080.0 nm)	H→L: 0.66 (667.7 nm)	3.2557
S-04	H→L: 0.67 (1109.4 nm)	H→L: 0.66 (685.7 nm)	2.6983
S-05	H→L: 0.59 (1089.3 nm)	H→L: 0.66 (716.2 nm)	2.9291

^aH→L represents the HOMO to LUMO transition. CI stands for configuration interaction.

Photovoltaic Properties

Photovoltaic performance characteristics of the OSCs are summarized in Table 3.

The optimized donor/acceptor ratio of **S-01** to **S-03** based devices is 1:1 w/w, while

the optimized donor/acceptor ratio of **S-04** and **S-05** based devices is 1:3 w/w. Figure 5 shows the J - V curves of the OSCs based on **S-01**:PC₆₀BM (1:1, w/w), **S-02**:PC₆₀BM (1:1, w/w), **S-03**:PC₆₀BM (1:1, w/w), **S-04**:PC₆₀BM (1:3, w/w) and **S-05**:PC₆₀BM (1:3, w/w) under the illumination of AM 1.5 G at 100 mW cm⁻². The PCE of the OSC based on **S-01**:PC₆₀BM (1:1, w/w) is 2.13%, with V_{oc} = 0.85 V, J_{sc} = 4.26 mA cm⁻² and FF = 0.589. Much lower J_{sc} (2.88 mA cm⁻²) and FF (0.455) were measured from **S-02**:PC₇₀BM (1:1, w/w) based OSC, leading to an overall decrease of PCE to 1.13%. By using ATVTA as the building block for π -conjugation extension in **S-03**, an elevated V_{oc} value of 0.96 V was achieved from **S-03**:PC₆₀BM (1:1, w/w) based device, with a higher PCE of 2.19%, a J_{sc} of 4.57 mA cm⁻² and a FF of 0.50. It is well known that V_{oc} is tightly correlated with the energy level difference between the HOMO of the donor and the LUMO of the acceptor. Furthermore, the morphology of active layer has also been demonstrated to have a noticeable effect on the V_{oc} .^[41] Thus, the more well-defined morphology probably is a factor that leads to higher V_{oc} of **S-03** based device than that of **S-01** and **S-02** based devices in this case.

Satisfactory V_{oc} values were also achieved from the **S-04** or **S-05** based devices. Device based on **S-04**:PC₆₀BM (1:3, w/w) exhibited a PCE of 1.02%, with a high V_{oc} of 0.98 V. The device based on **S-05**:PC₆₀BM (1:3, w/w) has a slightly higher V_{oc} of 0.98 V, with a enhanced J_{sc} of 4.48 mA cm⁻², leading to a PCE of 1.22%. The results indicate that the new unit ATVTA is a promising building block to guarantee the low-lying energy levels while extending π -conjugation of the molecules.

Table 3 The photovoltaic performance of the OSCs based on **S-01**, **S-02**, **S-03**, **S-04** or **S-05** as donor, PC₆₀BM as acceptor, under the illumination of AM 1.5 G at 100 mW cm⁻².

Active layer	V_{oc} [V]	J_{sc} [mA cm ⁻²]	FF	PCE [%]
S-01 :PC ₆₀ BM (1:1)	0.85	4.26	0.589	2.13
S-02 :PC ₆₀ BM (1:1)	0.86	2.88	0.455	1.13
S-03 :PC ₆₀ BM (1:1)	0.96	4.57	0.50	2.19
S-04 :PC ₆₀ BM (1:3)	0.98	3.40	0.308	1.02
S-05 :PC ₆₀ BM (1:3)	0.99	4.48	0.276	1.22

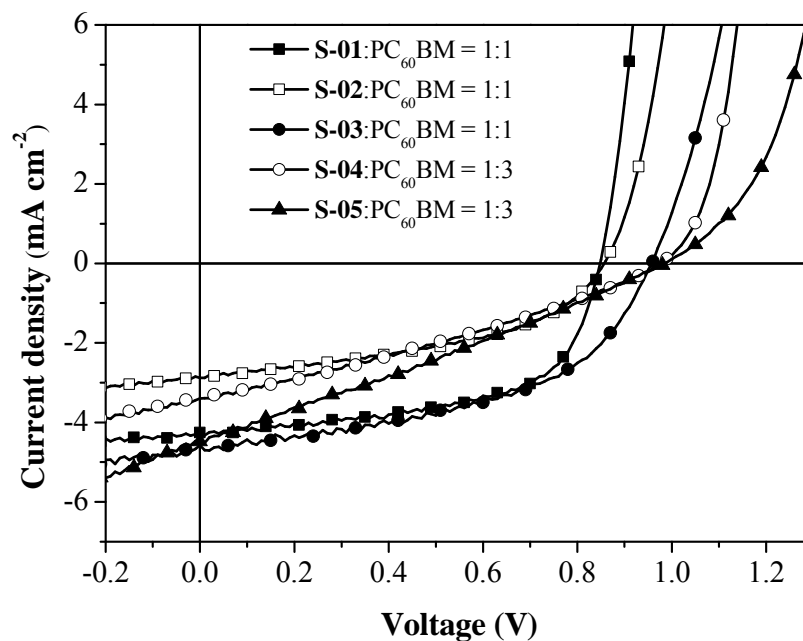


Figure 5 The J - V curve of the OSCs based on **S-01**:PC₆₀BM (1:1, w/w), **S-02**:PC₆₀BM (1:1, w/w), **S-03**:PC₆₀BM (1:1, w/w), **S-04**:PC₆₀BM (1:3, w/w) and **S-05**:PC₆₀BM (1:3, w/w) under the illumination of AM 1.5 G at 100 mW cm⁻².

The external quantum efficiency (EQE) of the OSCs based on **S-01**:PC₆₀BM (1:1, w/w), **S-02**:PC₆₀BM (1:1, w/w), **S-03**:PC₆₀BM (1:1, w/w), **S-04**:PC₆₀BM (1:3, w/w) and **S-05**:PC₆₀BM (1:3, w/w) are shown in Figure 6. The J_{sc} values derived from integration of the EQE curve are rather consistent (less than 5% error) with the values obtained by $J-V$ measurements. The maximum EQE value of the OSC based on **S-03**:PC₆₀BM (1:1, w/w) reached 35% at 543 nm. The maximum EQE values of the **S-03**, **S-04** and **S-05** based devices are ~28% at around 480 nm.

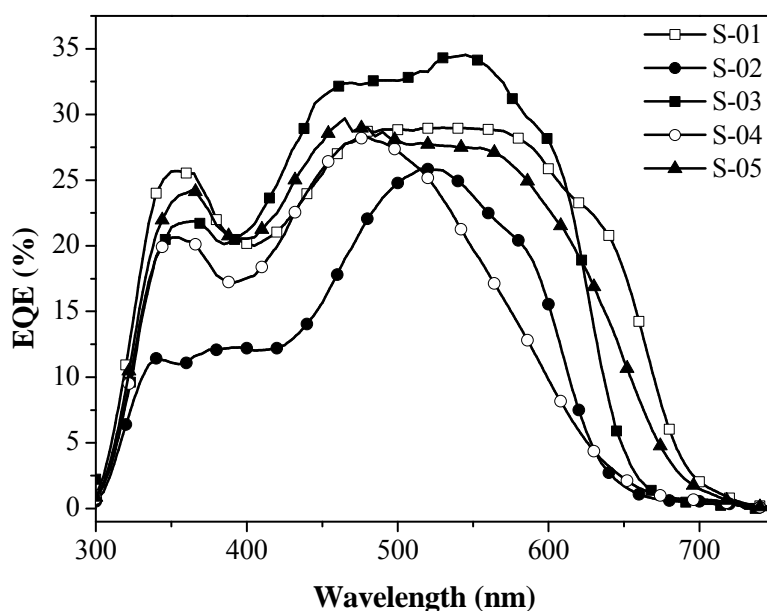


Figure 6 The EQE of the OSCs based on **S-01**:PC₆₀BM (1:1, w/w), **S-02**:PC₆₀BM (1:1, w/w), **S-03**:PC₆₀BM (1:1, w/w), **S-04**:PC₆₀BM (1:3, w/w) and **S-05**:PC₆₀BM (1:3, w/w).

Morphology Characterization

A nanoscale phase separation and bicontinuous donor/acceptor (D/A) interpenetrating network in the active layer is desirable for high efficiency charge

separation and transportation to get high photovoltaic performance. To better understand the morphology effect on the photovoltaic performance of the devices, the morphology of the active layer of **S-01**:PC₆₀BM (1:1, w/w), **S-02**:PC₆₀BM (1:1, w/w) and **S-03**:PC₆₀BM (1:1, w/w) was studied by transmission electron microscopy (TEM). As shown in Figure 7, the blend films of **S-01**:PC₆₀BM (1:1, w/w) and **S-03**:PC₆₀BM (1:1, w/w) gave a similar and better bicontinuous D/A interpenetrating network and relatively well-developed fibrillar structure, which should favor high efficiency exciton dissociation and charge transportation. While the blend film of **S-02**:PC₆₀BM (1:1, w/w) exhibited a larger domain size and a less defined phase separation, it would result in the overall lower photovoltaic performance of the **S-02** based OSCs.

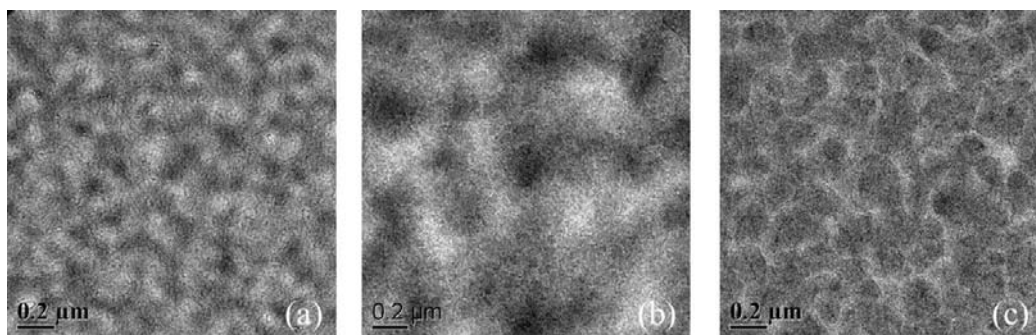
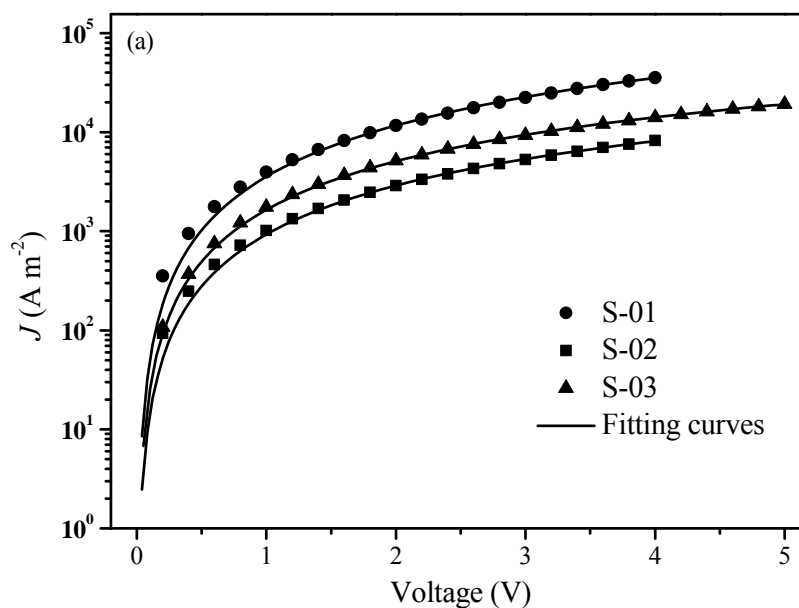


Figure 7 TEM images of the blend films of (a) **S-01**:PC₆₀BM (1:1, w/w), (b) **S-02**:PC₆₀BM (1:1, w/w) and (c) **S-03**:PC₆₀BM (1:1, w/w).

SCLC Mobilities

It is well known that a balanced charge-carrier transport is desirable for high FF.^[42] In order to investigate charge transport properties of the **S-01**:PC₆₀BM (1:1, w/w), **S-02**:PC₆₀BM (1:1, w/w) and **S-03**:PC₆₀BM (1:1, w/w) blend films, both the electron (μ_e) and hole mobilities (μ_h) were measured by using the space-charge-limited current

(SCLC) method.^[43] The corresponding blend film dependency of the hole and the electron mobilities are shown in Figure 8. The detailed hole and electron mobilities of the blend films of **S-01**:PC₆₀BM (1:1, w/w), **S-02**:PC₆₀BM (1:1, w/w) and **S-03**:PC₆₀BM (1:1, w/w) are summarized in Table 4. The same order of magnitude for the hole mobilities as well as electron mobilities of the blend films based on the three molecules was obtained, respectively. The blend film of **S-01**:PC₆₀BM exhibited more balanced μ_h and μ_e than those of **S-02**:PC₆₀BM and **S-03**:PC₆₀BM, resulting in the higher FF value of the corresponding OSCs obtained.



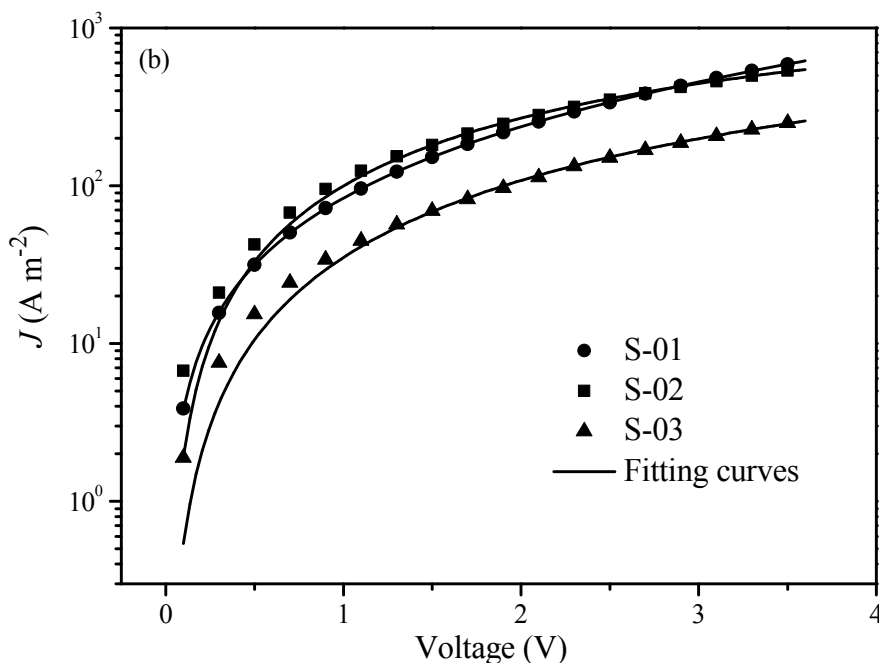


Fig. 8 The current-voltage plots of (a) the electron-only devices and (b) hole-only devices.

Table 4 Hole and electron mobilities of the blend films of **S-01**:PC₆₀BM (1:1, w/w), **S-02**:PC₆₀BM (1:1, w/w) and **S-03**:PC₆₀BM (1:1, w/w)

Blend films	μ_e (cm ² v ⁻¹ s ⁻¹)	μ_h (cm ² v ⁻¹ s ⁻¹)	μ_h / μ_e
S-01 :PC ₆₀ BM (1:1)	4.67×10^{-4}	1.34×10^{-3}	2.87
S-02 :PC ₆₀ BM (1:1)	5.53×10^{-4}	4.31×10^{-3}	7.79
S-03 :PC ₆₀ BM (1:1)	1.40×10^{-4}	1.02×10^{-3}	7.28

Conclusion

A new building block ATVTA which utilizes stiff carbon-carbon triple bonds as the linkage on TVT unit is developed. We have designed and synthesized three small molecules **S-01**, **S-02** and **S-03** with TVT, AT2 and ATVTA as the building unit,

respectively, to investigate their physicochemical and photovoltaic properties. **S-01**, **S-02** and **S-03** possess good solubility in common organic solvents, broad visible absorption at 350–650 nm and low-lying HOMO energy levels at -5.27 eV, -5.37 eV and -5.29 eV, respectively. The OSCs based on **S-01**:PC₆₀BM (1:1, w/w) and **S-02**:PC₆₀BM (1:1, w/w) exhibited a high V_{oc} of 0.85 V and 0.86 V, respectively. Especially, device based on **S-03** with ATVTA building block showed a higher V_{oc} of 0.96 V, with a PCE of 2.19%. The result indicates that ATVTA unit is a promising building block for extending π conjugation of the molecules without pushing up their HOMO energy levels. We changed the terminal unit of **S-03** by the strong electron-withdrawing groups to give **S-04** and **S-05**. The devices based on **S-04** and **S-05** exhibited a slightly higher V_{oc} of 0.98 V and 0.99 V, respectively. This present work demonstrates that the ATVTA building unit offers a good avenue toward designing new photovoltaic small molecule-based donor materials with high V_{oc} for OSCs.

Experimental Section

Physical Measurements

NMR spectra were measured in CDCl₃ on Bruker AV 400 MHz FT-NMR spectrometer and chemical shifts are quoted relative to tetramethylsilane for ¹H and ¹³C nuclei. The ¹H and ¹³C NMR spectra of **S-01** to **S-05** are shown in the Supporting Information, and the NMR data are consistent with the proposed structures. Thermogravimetric analysis (TGA) was performed on a Perkin-Elmer TGA-7. The

positive-ion fast atom bombardment (FAB) mass spectra were recorded in *m*-nitrobenzyl alcohol matrices on a Finnigan-MAT SSQ710 mass spectrometer and high resolution (HR) MALDI-TOF (matrix-assisted laser desorption ionization/time-of-flight) spectra were obtained by a Autoflex Bruker MALDI-TOF mass spectrometer. UV-vis absorption spectra were obtained on a Hitachi U-3010 spectrometer. Cyclic voltammetry was performed on a Zahner IM6e electrochemical workstation with a three-electrode system in a solution of 0.1 M Bu₄NPF₆ acetonitrile solution at a scan rate of 100 mV s⁻¹. Glassy carbon coated with the relevant compound as a thin film was used as the working electrode. A Pt wire was used as the counter electrode and Ag/Ag⁺ was used as the reference electrode. The geometries of the compounds were optimized using density functional theory (DFT) with B3LYP functional and 6-31G (d, p) basis set. In particular, the HOMO and LUMO energy levels and related electron distributions were calculated. The alkyl chains were replaced by methyl groups to save the computational time within a reasonable simplification.

Device Fabrication and Characterization of OSCs

OSCs were fabricated with ITO glass as a positive electrode, Ca/Al as a negative electrode and the blend films of the **S-01** to **S-05**/PC₆₀BM between them as a photosensitive layer. The ITO glass was pre-cleaned and modified by a thin layer of PEDOT:PSS which was spin-cast from a PEDOT:PSS aqueous solution on the ITO substrate, and the thickness of the PEDOT:PSS layer is about 30 nm. The

photosensitive layer, consisting of the donor material and fullerene derivative, was obtained by dissolving the mixture in the chloroform solvent and spin-coated on the ITO/PEDOT:PSS electrode. Finally, the Ca/Al cathode was deposited on the active layer by vacuum evaporation under 1×10^{-4} Pa. The effective area of the device is 4 mm^2 . The characterization of the current density-voltage (J - V) curve was done under an inert nitrogen atmosphere and the EQEs of the devices without encapsulation were measured in air.

Mobility Measurements

The hole and electron mobilities were calculated by using the space-charge-limited current (SCLC) method based on the following equation.^{43c}

$$J = \frac{9}{8} \varepsilon \varepsilon_0 \mu_0 V^2 \exp(0.89\sqrt{V/E_0L}) / L^3$$

where ε is the dielectric constant of the polymers, ε_0 is the permittivity of the vacuum, μ_0 is the zero-field mobility, E_0 is the characteristic field, J is the current density, and L is the thickness of the film.

Syntheses

2-Bromo-3-hexylthiophene (1)

A solution of 3-hexylthiophene (5 g) in chloroform and acetic acid (100 mL, 1:1, v/v) was stirred at 0 °C, and *N*-bromosuccinimide (5.56 g) was added in small portions. After being stirred for half an hour at room temperature, the reaction mixture was poured into water and extracted with CH_2Cl_2 . The organic layer was washed with water three times and dried over Na_2SO_4 . After the removal of solvent, the crude

product was purified by column chromatography on silica gel using hexane as eluent to afford compound **1** (7 g, yield: 95%) as a colorless oil.

^1H NMR (400 MHz, CDCl_3), δ (ppm): 7.18–7.17 (d, $J = 4$ Hz, 1H, Ar), 6.80–6.78 (d, $J = 8$ Hz, 1H, Ar), 2.58–2.54 (t, $J = 16$ Hz, 2H, alkyl), 1.59–1.54 (m, 2H, alkyl), 1.35–1.27 (m, 6H, alkyl), 0.90–0.87 (m, 3H, alkyl). ^{13}C NMR (100 MHz, CDCl_3), δ (ppm): 141.99, 128.25, 128.13, 108.82 (Ar), 31.66, 29.74, 29.43, 28.93, 22.63, 14.11 (alkyl). MALDI-TOF m/z 246.1 [$M-1$] $^+$.

5-Bromo-4-hexylthiophene-2-carbaldehyde (2)

Dry DMF (3 mL) was added dropwise to POCl_3 (4 mL) and the mixture was stirred at 0 °C under argon. After stirring at 0 °C for half an hour, 4 g of 2-bromo-3-hexylthiophene (**1**) (16.2 mmol) in 1,2-dichloroethane (30 mL) was added to the mixture which was stirred at 90 °C for 12 h. Then the mixture was poured into ice water (200 mL), neutralized with NaHCO_3 and then extracted with CH_2Cl_2 . The organic layer was washed with water three times and dried over Na_2SO_4 . After the removal of solvent, the residue was chromatographed on silica gel using a mixture of hexane and dichloromethane (5:1) as eluent to afford the target product as a light yellow oil (3 g, yield: 67%).

^1H NMR (400 MHz, CDCl_3), δ (ppm): 9.75 (s, 1H, CHO), 7.46 (s, 1H, Ar), 2.61–2.57 (t, $J = 16$ Hz, 2H, alkyl), 1.62–1.56 (m, 2H, alkyl), 1.36–1.29 (m, 6H, alkyl), 0.90–0.87 (m, 3H, alkyl). ^{13}C NMR (100 MHz, CDCl_3), δ (ppm): 181.85 (CHO), 143.99, 142.90, 136.81, 108.82 (Ar), 31.66, 29.74, 29.43, 28.93, 22.63, 14.11 (alkyl).

MALDI-TOF: m/z 276.0 $[M+1]^+$.

3,4'-Dihexyl-(2,2'-bithiophene)-5-carbaldehyde (3)

5-Bromo-4-hexylthiophene-2-carbaldehyde (**2**) (3 g, 10.8 mmol) and 2-(tributylstannyl)-4-octylthiophene (5.7 g, 13 mmol) were charged into a flask with 50 mL toluene, the solution was flushed with nitrogen for 10 min, and 100 mg of Pd(PPh₃)₄ was added. The solution was flushed again for 10 min. After being stirred at 110 °C for 24 h under nitrogen protection, the reaction mixture was poured into water (100 mL) and extracted with CH₂Cl₂. The organic layer was washed with water and dried over Na₂SO₄. After the removal of solvent, the crude product was purified by column chromatography on silica gel using a mixture of hexane and dichloromethane (5:1) as eluent to afford compound **3** (3.4 g, yield: 85%) as a light yellow oil.

¹H NMR (400 MHz, CDCl₃), δ (ppm): 9.82 (s, 1H, CHO), 7.57 (s, 1H, Ar), 6.96 (s, 1H, Ar), 2.76–2.72 (t, 2H, alkyl), 2.59–2.55 (t, 2H, alkyl), 1.69–1.56 (m, 4H, alkyl), 1.42–1.26 (m, 12H, alkyl), 0.91–0.87 (m, 6H, alkyl). ¹³C NMR (100 MHz, CDCl₃), δ (ppm): 182.49 (CHO), 144.11, 141.74, 140.11, 138.97, 134.61, 128.82, 122.17 (Ar), 31.68, 31.62, 30.38, 30.29, 29.30, 29.16, 29.04, 28.89, 22.69, 22.63, 14.14, 14.10 (alkyl). MALDI-TOF: m/z 362.2 $[M]^+$.

5'-Bromo-3,4'-dihexyl-(2,2'-bithiophene)-5-carbaldehyde (4)

A solution of 3,4'-dihexyl-(2,2'-bithiophene)-5-carbaldehyde (**3**) (3.4 g 9.4 mmol) in

chloroform and acetic acid (100 mL, 1:1, v/v) was stirred at 0 °C, *N*-bromosuccinimide (1.84 g, 10.3 mmol) was added in small portions. After being stirred for 12 h at room temperature, the reaction mixture was poured into water and extracted with CH₂Cl₂. The organic layer was washed with water three times and dried over Na₂SO₄. After the removal of solvent, the crude product was purified by column chromatography on silica gel using hexane as eluent to afford compound **4** (3.7 g, yield: 90%) as a yellow oil.

¹H NMR (400 MHz, CDCl₃), δ (ppm): 9.82 (s, 1H, CHO), 7.57 (s, 1H, Ar), 6.96 (s, 1H, Ar), 2.76–2.72 (t, 2H, alkyl), 2.59–2.55 (t, 2H, alkyl), 1.69–1.56 (m, 4H, alkyl), 1.42–1.26 (m, 12H, alkyl), 0.91–0.87 (m, 6H, alkyl). ¹³C NMR (100 MHz, CDCl₃), δ (ppm): 182.52 (CHO), 142.97, 140.52, 140.49, 140.43, 138.82, 134.35, 128.27, 111.22 (Ar), 31.61, 31.52, 30.31, 29.28, 29.12, 28.90, 22.69, 22.62, 14.16, 14.12 (alkyl). MALDI-TOF: *m/z* 442.0 [*M*+1]⁺.

3,4'-Dihexyl-5'-((trimethylsilyl)ethynyl)-(2,2'-bithiophene)-5-carbaldehyde (**5**)

To a solution (50 mL) of compound **4** (2 g, 4.5 mmol) in NEt₃ and CH₂Cl₂ (1:1, v/v) was added a catalytic amount of CuI and Pd(PPh₃)₄ (0.2 g) under nitrogen. After stirring for 30 min at room temperature, trimethylsilylacetylene (1.76 g, 18 mmol) was added and then the mixture was stirred overnight at 60 °C. The reaction mixture was dried and the crude product was purified by column chromatography on silica gel using hexane and dichloromethane (1:1, v/v) as eluent to give compound **5** (1.5 g, yield: 78%) as a yellow oil. ¹H NMR (400 MHz, CDCl₃), δ (ppm): 9.81 (s, 1H, CHO),

7.56 (s, 1H, Ar), 7.01 (s, 1H, Ar), 2.79–2.75 (t, $J = 16$ Hz, 2H, alkyl), 2.70–2.66 (m, 4H, alkyl), 1.42–1.26 (m, 12H, alkyl), 0.91–0.86 (m, 6H, alkyl), 0.26 (s, 9H, alkyl). ^{13}C NMR (100 MHz, CDCl_3), δ (ppm): 182.48 (H, alkyl), CHO), 149.65, 140.89, 140.53, 140.44, 138.88, 134.96, 128.17, 119.01 (Ar), 85.38, 76.07 ($\text{C}\equiv\text{C}$), 31.60, 30.26, 30.09, 29.46, 29.43, 29.15, 28.93, 22.69, 22.61, 14.15, 14.11, 14.08, 3.40 (alkyl). MALDI-TOF: m/z 458.2 $[M]^+$.

5'-Ethynyl-3,4'-dihexyl-(2,2'-bithiophene)-5-carbaldehyde (6)

Compound **5** (1.5 g, 3.4 mmol) and K_2CO_3 (0.5 g, 3.7 mmol) were dissolved in a solvent mixture of MeOH and CH_2Cl_2 (1:1, v/v). The mixture was stirred for 6 h at room temperature. It was poured into water and extracted with CH_2Cl_2 . The organic layer was washed with water three times and then dried over Na_2SO_4 . After the removal of solvent, the crude product was purified by column chromatography on silica gel using hexane and dichloromethane (1:1, v/v) as eluent to afford compound **6** (0.78 g, yield: 60%) as a yellow oil.

^1H NMR (400 MHz, CDCl_3), δ (ppm): 9.82 (s, 1H, CHO), 7.57 (s, 1H, Ar), 7.03 (s, 1H, Ar), 3.56 (s, 1H, $\text{C}\equiv\text{CH}$), 2.79–2.75 (t, $J = 16$ Hz, 2H, alkyl), 2.72–2.68 (t, $J = 16$ Hz, 2H, alkyl), 1.69–1.60 (m, 4H, alkyl), 1.42–1.26 (m, 12H, alkyl), 0.91–0.86 (m, 6H, alkyl). ^{13}C NMR (100 MHz, CDCl_3), δ (ppm): 182.48 (CHO), 149.65, 140.89, 140.53, 140.44, 138.88, 134.96, 128.17, 119.01 (Ar), 85.38, 76.07 ($\text{C}\equiv\text{C}$). 31.71, 31.55, 30.21, 29.48, 29.13, 28.70, 22.67, 22.62, 14.16, 14.12 (alkyl), MALDI-TOF: m/z 386.1 $[M]^+$.

(E)-1,2-Bis(2-thienyl)ethylene (7)

TiCl₄ (2.26 mL, 15 mmol) was added dropwise to a stirred suspension of zinc powder (1.96 g, 30 mmol) in dry THF (100 mL) at -10 °C under the protection of nitrogen. The resulting dark mixture was heated under reflux for 1 h. The suspension was cooled to room temperature and 2-formylthiophene (1.76 g, 15.6 mmol) was added slowly. Reflux was continued for 4 h under nitrogen. The resulting mixture was poured into 10% aqueous K₂CO₃ solution (200 mL) and the aqueous layer was extracted with Et₂O. The organic layer was washed with water three times and then dried over Na₂SO₄. After the removal of solvent, the crude product was purified by column chromatography on silica gel using hexane as eluent to afford compound **7** (1.2 g, yield: 80%) as a yellow powder.

¹H NMR (400 MHz, CDCl₃), δ (ppm): 7.19–7.17 (m, 2H, Ar), 7.05–7.03 (m, 4H, Ar), 7.00–6.98 (m, 2H, CH=CH). ¹³C NMR (100 MHz, CDCl₃), δ (ppm): 141.81 (Ar), 136.40 (C=C), 130.53, 129.18, 128.43 (Ar). MALDI-TOF: *m/z* 192.0 [*M*]⁺.

(E)-1,2-Bis(5-iodothiophen-2-yl)ethylene (8)

A solution of compound **7** (0.5 g, 2.6 mmol) in chloroform and acetic acid (100 mL, 1:1, v/v) was stirred at 0 °C, and *N*-iodosuccinimide (1.28 g, 5.7 mmol) was added in small portions. After being stirred for 2 h at room temperature, the reaction mixture was poured into water and extracted with CH₂Cl₂. The organic layer was washed with water three times and dried over Na₂SO₄. After the removal of solvent, the crude product was purified by column chromatography on silica gel using hexane as eluent

to afford compound **8** (1 g, yield: 85%) as a yellow powder.

^1H NMR (400 MHz, CDCl_3), δ (ppm): 7.14–7.13 (d, $J = 4$ Hz, 2H, Ar), 6.87–6.86 (d, $J = 4$ Hz, 2H, Ar), 6.70–6.69 (d, $J = 4$ Hz, 2H, CH=CH). ^{13}C NMR (100 MHz, CDCl_3), δ (ppm): 147.93, 137.66 (Ar), 127.78 (C=C), 121.21, 72.75 (Ar). MALDI-TOF: m/z 443.8 $[M]^+$.

(E)-1,2-Bis(5-(tributylstannyl)thiophen-2-yl)ethylene (9)

Compound **8** (1 g, 5.2 mmol) and 60 mL of dry THF were added into a flask under nitrogen protection. The solution was cooled to -78 °C and 4.6 mL *n*-butyllithium (11 mmol, 2.4 M in *n*-hexane) was added dropwisely. After the reaction mixture was stirred at -78 °C for 2 h, tributyltin chloride (13 mmol, 3.6 mL) was added in one portion. Then the mixture was stirred at ambient temperature for 24 h. The reaction mixture was poured into water and extracted with CH_2Cl_2 . The organic layer was washed with water three times and then dried over Na_2SO_4 . After the removal of solvent, the crude product was used for next step without any purification.

5,5'-Diiodo-2,2'-bithiophene (10)

Compound **10** was synthesized similarly as described above for compound **8** except that 2,2'-bithiophene was used instead of compound **7**. (1.1 g yield: 86%, white solid).

^1H NMR (400 MHz, CDCl_3), δ (ppm): 7.15–7.14 (d, $J = 4$ Hz, 2H, Ar), 6.79–6.78 (d, $J = 4$ Hz, 2H, Ar). ^{13}C NMR (100 MHz, CDCl_3), δ (ppm): 142.07, 137.69, 125.54, 72.60 (Ar). MALDI-TOF: m/z 417.8 $[M]^+$.

(E)-5'',5''''-(Ethene-1,2-diyl)bis(3,4'-dihexyl-[2,2':5',2''-terthiophene]-5-carbaldehyde)

(11)

Compounds **4** (0.5 g, 1.1 mmol) and **9** (0.41 g, 0.5 mmol) were put into a flask with toluene (50 mL), and the solution was flushed with nitrogen for 10 min. Then, 28 mg of Pd(PPh₃)₄ (0.024 mmol) was added. The solution was flushed again for 10 min. After being stirred at 110 °C for 24 h under nitrogen, the reaction mixture was poured into water (100 mL) and extracted with CH₂Cl₂. The organic layer was further washed with water and dried over Na₂SO₄. After the removal of solvent, the crude product was purified by column chromatography on silica gel using a mixture of hexane and dichloromethane (5:1, v/v) as eluent to afford compound **11** (0.37 g, yield: 78%) as a red solid.

¹H NMR (400 MHz, CDCl₃), δ (ppm): 9.83 (s, 2H, CHO), 7.59 (s, 2H, Ar), 7.13 (s, 2H, Ar), 7.09–7.08 (d, *J* = 4 Hz, 2H, CH=CH), 7.03–7.02 (d, *J* = 4 Hz, 4H, Ar), 2.85–2.79 (m, 8H, alkyl), 1.73–1.66 (m, 8H, alkyl), 1.42–1.25 (m, 24H, alkyl), 0.92–0.88 (m, 12H, alkyl). ¹³C NMR (100 MHz, CDCl₃), δ (ppm): 182.42 (CHO), 148.32, 143.68, 141.63, 139.17, 138.62, 138.18, 138.03, 137.56, 137.11 (Ar), 136.45 (C=C), 132.56, 130.18, 126.32 (Ar), 32.29, 32.27, 31.87, 31.83, 28.97, 28.94, 28.60, 28.32, 22.78, 22.76, 14.17, 14.16 (alkyl). MALDI-TOF: *m/z* 912.32 [*M*-1]⁺.

Synthesis of **S-01**

Compound **11** (130 mg, 0.14 mmol) was dissolved in a solution of dry CHCl₃ (50 mL)

and three drops of triethylamine followed by octyl cyanoacetate (0.6 ml, 2.8 mmol) were added and the resulting solution was stirred for 40 h under nitrogen at room temperature. The reaction mixture was then extracted with CH₂Cl₂, washed with water and dried over Na₂SO₄. After the removal of solvent, the residue was purified on silica gel column using a mixture of dichloromethane and petroleum ether (1:1, v/v) as the eluent to afford **S-01** as a brown solid (147 mg, yield: 83%).

¹H NMR (400 MHz, CDCl₃), δ (ppm): 8.20 (s, 2H, C=CH), 7.56 (s, 2H, Ar), 7.19 (s, 2H, Ar), 7.09–7.08 (d, *J* = 4 Hz, 2H, CH=CH), 7.04–7.03 (d, *J* = 4 Hz, 4H, Ar), 4.31–4.27 (t, *J* = 16 Hz, 4H, alkyl), 2.85–2.79 (m, 8H, alkyl), 1.79–1.65 (m, 12H, alkyl), 1.42–1.29 (m, 44H, alkyl), 0.93–0.87 (m, 18H, alkyl). ¹³C NMR (100 MHz, CHCl₃): δ 163.15 (O–C=O), 146.01 (C=C), 142.67, 141.81, 141.05, 140.50, 140.38, 133.53, 132.74 (Ar), 132.32 (C=C), 130.94, 127.06, 126.72, 121.32 (Ar), 116.05 (–C≡N), 97.47 (C=C), 66.54, 31.77, 31.64, 31.60, 30.43, 30.11, 29.47, 29.32, 29.28, 29.17, 28.55, 25.79, 22.64, 22.61, 14.12, 14.10 (Ar). MALDI-TOF: *m/z* 1270.57 [*M*]⁺. Elemental anal. (%) calcd for C₇₄H₉₈N₂O₄S₆: C 69.88, H 7.77, N 2.20; found: C 70.02, H 7.93, N 2.30.

5',5'''-([2,2'-Bithiophene]-5,5'-diylbis(ethyne-2,1-diyl))bis(3,4'-dihexyl-[2,2'-bithiophene]-5-carbaldehyde) (12)

Compounds **6** (0.21 g, 0.54 mmol) and **10** (0.1 g, 0.25 mmol) were put into a flask with 40 mL of THF/NEt₃ (1:1, v/v), and the solution was flushed with nitrogen for 10 min. Then, 15 mg of Pd(PPh₃)₄ (0.013 mmol) and 2 mg of CuI (0.01 mmol) were

added. The solution was flushed again for 10 min. After being stirred at 50 °C for 24 h under nitrogen, the reaction mixture was poured into water (100 mL) and extracted with CH₂Cl₂. The organic layer was washed with water and dried over Na₂SO₄. After the removal of solvent, the crude product was purified by column chromatography on silica gel using a mixture of hexane and dichloromethane (1:2) as eluent to afford compound **12** as a red solid (145 mg, yield: 65%).

¹H NMR (400 MHz, CDCl₃), δ (ppm): 9.83 (s, 2H, CHO), 7.59 (s, 2H, Ar), 7.20–7.19 (d, *J* = 4 Hz, 2H, Ar), 7.12–7.11 (d, *J* = 4 Hz, 2H, Ar), 7.09 (s, 2H, Ar), 2.83–2.72 (m, 8H, alkyl), 1.72–1.64 (m, 8H, alkyl), 1.41–1.26 (m, 24H, alkyl), 0.92–0.88 (m, 12H, alkyl). ¹³C NMR (100 MHz, CDCl₃), δ (ppm): 182.50 (CHO), 149.00, 140.84, 140.62, 140.43, 138.99, 138.43, 135.45, 132.98, 128.47, 124.21, 122.25, 119.76 (Ar), 90.38, 87.18 (C≡C), 31.64, 31.62, 30.25, 30.14, 29.66, 29.54, 29.20, 28.93, 22.65, 22.64, 14.16, 14.12 (alkyl). MALDI-TOF: *m/z* 934.32 [*M*]⁺.

Synthesis of **S-02**

S-02 was synthesized similarly as described above for **S-01** except that compound **12** (145 mg, 0.15 mmol) was used instead of compound **11** (160 mg, yield: 80%).

¹H NMR (400 MHz, CDCl₃), δ (ppm): 8.21 (s, 2H, C=CH), 7.56 (s, 2H, Ar), 7.20–7.19 (d, *J* = 4 Hz, 2H, Ar), 7.15 (s, 2H, Ar), 7.12–7.11 (d, *J* = 4 Hz, 2H, Ar), 4.31–4.27 (t, *J* = 16 Hz, 4H, alkyl), 2.85–2.72 (m, 8H, alkyl), 1.75–1.65 (m, 12H, alkyl), 1.39–1.29 (m, 44H, alkyl), 0.92–0.87 (m, 18H, alkyl). ¹³C NMR (100 MHz, CHCl₃): δ 163.05 (O=C=O), 149.13 (C=C), 145.97, 141.28, 140.95, 140.91, 138.49,

135.02, 133.15, 133.04, 128.88, 124.25, 122.23, 120.21 (Ar), 115.96 ($-\text{C}\equiv\text{N}$), 98.02 ($\text{C}=\text{C}$), 90.73, 87.22 ($\text{C}\equiv\text{C}$), 66.62, 31.77, 31.58, 30.15, 29.63, 29.38, 29.18, 29.16, 28.94, 28.55, 25.80, 22.65, 22.61, 14.13, 14.10, 14.08 (alkyl). MALDI-TOF: m/z 1292.59 $[M]^+$. Elemental anal. (%) calcd for $\text{C}_{76}\text{H}_{96}\text{N}_2\text{O}_4\text{S}_6$: C 70.55, H 7.48, N 2.16; found: C 70.70, H 7.58, N 2.21.

(E)-5',5'''-((5,5'-(Ethene-1,2-diyl)bis(thiophene-5,2-diyl))bis(ethyne-2,1-diyl))bis(3,4'-dihexyl-[2,2'-bithiophene]-5-carbaldehyde) (**13**)

Compound **13** was synthesized similarly as described above for compound **12** except that compound **8** (0.1 g, 0.22 mmol) was used instead of compound **10** (126 mg, yield: 58%).

^1H NMR (400 MHz, CDCl_3), δ (ppm): 9.83 (s, 2H, CHO), 7.59 (s, 2H, Ar), 7.17–7.16 (d, $J = 4$ Hz, 2H, Ar), 7.09 (s, 2H, $\text{CH}=\text{CH}$), 6.98–6.97 (t, $J = 4$ Hz, 4H, Ar), 2.83–2.72 (m, 8H, alkyl), 1.72–1.64 (m, 8H, alkyl), 1.41–1.26 (m, 24H, alkyl), 0.92–0.87 (m, 12H, alkyl). ^{13}C NMR (100 MHz, CDCl_3), δ (ppm): 182.50 (CHO), 148.91, 144.06, 140.81, 140.67, 140.40, 139.00, 135.36, 132.88, 128.47 (Ar), 126.92 ($\text{C}=\text{C}$), 121.83, 119.89, 119.02 (Ar), 91.01, 87.18 ($\text{C}\equiv\text{C}$), 31.62, 30.25, 30.14, 29.66, 29.54, 29.20, 28.94, 28.91, 22.65, 22.64, 14.16, 14.12 (alkyl). MALDI-TOF: m/z 960.32 $[M]^+$.

Synthesis of **S-03**

S-03 was synthesized similarly as described above for **S-01** except that compound **13**

(126 mg, 0.13 mmol) was used instead of compound **11** (147 mg, yield: 85%).

^1H NMR (400 MHz, CDCl_3), δ (ppm): 8.21 (s, 2H, C=CH), 7.56 (s, 2H, Ar), 7.17–7.15 (t, $J = 8$ Hz, 4H, Ar), 6.99–6.97 (m, 4H, Ar, CH=CH), 4.31–4.27 (t, $J = 16$ Hz, 4H, alkyl), 2.83–2.72 (m, 8H, alkyl), 1.77–1.65 (m, 12H, alkyl), 1.39–1.29 (m, 44H, alkyl), 0.92–0.87 (m, 18H, alkyl). ^{13}C NMR (100 MHz, CHCl_3): δ 163.06 (O–C=O), 149.05 (C=C), 145.99, 144.13, 141.34, 140.91, 134.94, 133.12 (Ar), 132.94 (C=C), 128.89, 126.97, 121.87, 121.79, 120.34, 115.99 (Ar), 113.03 (–C \equiv N), 97.98 (C=C), 91.37, 87.23 (C \equiv C), 67.19, 66.63, 31.80, 31.76, 31.61, 30.18, 30.16, 29.65, 29.41, 29.21, 29.19, 29.14, 28.98, 28.58, 28.35, 25.83, 25.72, 24.78, 22.68, 22.65, 22.64, 14.17, 14.14, 14.12 (alkyl). MALDI-TOF: m/z 1318.57 [M] $^+$. Elemental anal. (%) calcd for $\text{C}_{78}\text{H}_{98}\text{N}_2\text{O}_4\text{S}_6$: C 70.97, H 7.48, N 2.12; found: C 71.10, H 7.75, N 2.35.

Synthesis of **S-04**

Compound **13** (180 mg, 0.187 mmol) was dissolved in a solution of dry CHCl_3 (50 mL) and three drops of pyridine followed by malononitrile (0.123 g, 1.87 mmol) were added and the resulting solution was stirred for 12 h under nitrogen at room temperature. The reaction mixture was then extracted with CH_2Cl_2 , washed with water and dried over Na_2SO_4 . After the removal of solvent, the residue was purified on silica gel column using a mixture of CH_2Cl_2 and petroleum ether (1:1, v/v) as the eluent to afford **S-04** as a brown solid (121 mg, yield: 61%).

^1H NMR (400 MHz, CDCl_3), δ (ppm): 7.69 (s, 2H, C=CH), 7.52 (s, 2H, Ar),

7.18–7.17 (m, 4H, Ar), 6.99–6.98 (d, $J = 4$ Hz, 4H, C=CH), 2.83–2.72 (m, 8H, alkyl), 1.70–1.32 (m, 32H, alkyl), 1.92–0.89 (m, 12H, alkyl). ^{13}C NMR (100 MHz, CHCl_3), δ (ppm): 182.49 (C=C), 149.84 (C=C), 149.11, 141.66, 141.15, 138.93, 133.07, 132.86, 132.32, 129.41, 128.47, 126.95, 126.88, 121.89 (Ar), 114.24 (C \equiv CN), 113.35 (C \equiv CN), 91.86 (C \equiv C), 86.99 (C \equiv C), 76.36 (C=C), 31.53, 30.20, 30.10, 30.00, 29.58, 29.47, 29.31, 29.11, 28.90, 28.87, 22.58, 14.08(alkyl). MALDI-TOF: m/z 1056.35 [M] $^+$. Elemental anal. (%) calcd for $\text{C}_{62}\text{H}_{64}\text{N}_4\text{S}_6$: C 70.41, H 6.10, N 5.30; found: C 70.56, H 6.21, N 5.35.

Synthesis of **S-05**

Compound **13** (180 mg, 0.187 mmol) was dissolved in a solution of dry CHCl_3 (50 mL) and three drops of triethylamine followed by 1,3-diethyl-2-thiobarbituric acid (0.748 mg, 3.74 mmol) were added and the resulting solution was stirred for 12 h under nitrogen at room temperature. The reaction mixture was then extracted with CH_2Cl_2 , washed with water and dried over Na_2SO_4 . After the removal of solvent, the residue was purified on silica gel column using a mixture of CH_2Cl_2 and petroleum ether (1:1, v/v) as eluent to afford **S-05** as a brown solid (142 mg, yield: 54%).

^1H NMR (400 MHz, CDCl_3), δ (ppm): 8.58 (s, 2H, C=CH), 7.69 (s, 2H, Ar), 7.35 (s, 2H, Ar), 7.18–7.17 (d, $J = 4$ Hz, 2H, C=CH), 6.99–6.98 (d, $J = 4$ Hz, 2H, C=CH), 4.62–4.56 (m, 8H, alkyl), 2.87–2.74 (m, 8H, alkyl), 1.72–1.32 (m, 32H, alkyl), 0.93–0.89 (m, 24H, alkyl). ^{13}C NMR (100 MHz, CHCl_3), δ (ppm): 178.59 (C=S), 160.97 (C=O), 159.87, 148.88 (C=C), 148.82, 144.19, 141.09 (C=C), 135.30, 134.76,

132.97, 129.47, 129.24, 126.95 121.87 (C=C), 110.05 (Ar), 91.90 (C≡C), 87.32 (C≡C), 43.94, 43.11, 31.56, 30.22, 30.16, 29.91, 29.60, 29.30, 29.14, 26.93, 22.58, 14.09, 14.04, 12.50, 12.36 (alkyl). MALDI-TOF: m/z 1324.41 $[M]^+$. Elemental anal. (%) calcd for $C_{72}H_{84}N_4O_4S_8$: C 65.22, H 6.39, N 4.23; found: C 65.20, H 6.55, N 4.30.

Acknowledgements

We thank the Hong Kong Research Grants Council (HKBU 203313) and the Hong Kong Polytechnic University for financial support. The work described in this paper was also partially supported by a grant from the Research Grants Council of the Hong Kong Special Administrative Region, China (Project No. T23-713/11) and HKBU Strategic Development Fund (SDF13-0531-A02). We also thank the Inter-institutional Collaborative Research Scheme (RC-ICRS/15-16/02) and the Key R&D Project of Shanxi Province (International cooperation program, No. 201603D421032) for the financial support.

References

- [1] G. Li, R. Zhu, Y. Yang, *Nat. Photonics* **2012**, *6*, 153–161.
- [2] J. W. Chen, Y. Cao, *Acc. Chem. Res.* **2009**, *42*, 1709–1718.
- [3] A. J. Heeger, *Adv. Mater.* **2014**, *26*, 10–27.
- [4] Y. F. Li, *Acc. Chem. Res.* **2012**, *45*, 732–733.
- [5] G. Yu, J. Gao, J. Hummelen, F. Wudl, A. J. Heeger, *Science* **1995**, *270*, 1789–1791.

- [6] Y. Lin, Y. Li, X. Zhan, *Chem. Soc. Rev.* **2012**, *41*, 4245–4272.
- [7] L. Ye, S. Zhang, L. Huo, M. Zhang, J. Hou, *Acc. Chem. Res.* **2014**, *47*, 1595–1603.
- [8] Z.-G. Zhang, Y. Li, *Sci. China Chem.* **2015**, *58*, 192–209.
- [9] a) C. Cui, W.-Y. Wong, Y. Li, *Energy Environ. Sci.* **2014**, *7*, 2276–2284; b) C. Cui, Z. He, Y. Wu, X. Cheng, H. Wu, Y. Li, Y. Cao, W.-Y. Wong, *Energy Environ. Sci.*, **2016**, *9*, 885–891; c) C. Cui, X. Guo, J. Min, B. Guo, X. Cheng, M. Zhang, C. J. Brabec, Y. Li, *Adv. Mater.* **2015**, *27*, 7469–7475.
- [10] H. Yao, L. Ye, B. Fan, L. Huo, J. Hou, *Sci. China Mater.* **2015**, *58*, 213–222.
- [11] X. Cheng, Q. Wan, Y. Wu, B. Guo, X. Guo, Y. Li, M. Zhang, C. Cui, Y. Li, *Sol. Energy Mater. Sol. Cells* **2016**, *149*, 162–169.
- [12] Y. Liu, J. Zhao, Z. Li, C. Mu, W. Ma, H. Hu, K. Jiang, H. Lin, H. Ade, H. Yan, *Nat. Commun.* **2014**, *5*, 5293.
- [13] Y. Chen, X. Wan, G. Long, *Acc. Chem. Res.* **2014**, *46*, 2645–2655.
- [14] Q. Zhang, B. Kan, F. Liu, G. Long, X. Wan, X. Chen, Y. Zuo, W. Ni, H. Zhang, M. Li, Z. Hu, F. Huang, Y. Cao, Z. Liang, M. Zhang, T. P. Russell, Y. Chen, *Nat. Photonics* **2015**, *9*, 35–41.
- [15] B. Kan, Q. Zhang, M. Li, X. Wan, W. Ni, G. Long, Y. Wang, X. Yang, H. Feng, Y. Chen, *J. Am. Chem. Soc.* **2014**, *136*, 15529–15532.
- [16] B. Kan, M. Li, Q. Zhang, F. Liu, X. Wan, Y. Wang, W. Ni, G. Long, X. Yang, H. Feng, Y. Zuo, M. Zhang, F. Huang, Y. Cao, T. P. Russell, Y. Chen, *J. Am. Chem. Soc.* **2015**, *137*, 3886–3893.

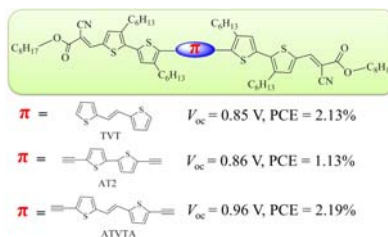
- [17] Y. Li, *Chem. Asian J.* **2013**, *8*, 2316–2328.
- [18] Y.-Y. Cheng, S.-H. Yang, C.-S. Hsu, *Chem. Rev.* **2009**, *109*, 5868–5923.
- [19] Y. Liang, L. Yu, *Polym. Rev.* **2010**, *50*, 454–473.
- [20] F. Zhang, D. Wu, Y. Xu, X. Feng, *J. Mater. Chem.* **2011**, *21*, 17590–17600.
- [21] A. Mishra, P. Bäuerle, *Angew. Chem. Int. Ed.* **2012**, *51*, 2020–2067.
- [22] C. Wang, H. Dong, W. Hu, Y. Liu, D. Zhu, *Chem. Rev.* **2011**, *112*, 2208–2267.
- [23] A. Facchetti, *Chem. Mater.* **2011**, *23*, 733–758.
- [24] A. Mishra, C.-Q. Ma, P. Bäuerle, *Chem. Rev.* **2009**, *109*, 1141–1276.
- [25] P. M. Beaujuge, J. J. Fréchet, *J. Am. Chem. Soc.* **2011**, *133*, 20009–20029.
- [26] C. Cui, J. Min, C.-L. Ho, T. Ameri, P. Yang, J. Zhao, C. J. Brabec, W.-Y. Wong, *Chem. Commun.* **2013**, *49*, 4409–4411.
- [27] X. M. Wu, J. Y. Wu, Y. Q. Liu, A. K. Y. Jen, *Chem. Commun.* **1999**, 2391–2392.
- [28] J. Casaso, T. M. Pappenfus, L. L. Miller, K. R. Mann, E. Orti, P. M. Viruela, R. Pou-Amerigo, V. Hernandez, J. T. L. Navarrete, *J. Am. Chem. Soc.* **2003**, *125*, 2524–2534.
- [29] Y. Liu, X. Wan, F. Wang, J. Zhou, G. Long, J. Tian, Y. Chen, *Adv. Mater.* **2011**, *23*, 5387–5391.
- [30] J. Hou, Z. Tan, Y. Yan, Y. He, C. Yang, Y. Li, *J. Am. Chem. Soc.* **2006**, *128*, 4911–4916.
- [31] a) Y. Li, Y. Zou, *Adv. Mater.* **2008**, *20*, 2952–2958; b) L. Gao, J. Zhang, C. He, S. Shen, Y. Zhang, H. Liu, Q. Sun, Y. Li, *Sci. China Chem.* **2013**, *56*, 997–1003; c) L. Gao, J. Zhang, C. He, Y. Zhang, Q. Sun, Y. Li, *Sci. China Chem.* **2014**, *57*, 966–972.

- [32] S. Liu, C.-C. Chen, Z. Hong, J. Gao, Y. Yang, H. Zhou, L. Dou, G. Li, Y. Yang, *Sci. Rep.* **2013**, *3*, 3356.
- [33] K. Sun, Z. Xiao, S. Lu, W. Zajaczkowski, W. Pisula, E. Hanssen, J. M. White, R. M. Williamson, J. Subbiah, J. Ouyang, A. B. Holmes, W. W. H. Wong, D. J. Jones. *Nat. Commun.* 2015, *6*, 6013.
- [34] H. Sirringhaus, *Nat. Mater.* **2003**, *2*, 641–642.
- [35] W. Kowalsky, E. Becker, T. Benstem, H.-H. Johannes, D. Metzdorf, H. Neuner, J. Schobel, *Adv. Solid State Phys.* **2000**, *40*, 795.
- [36] G. Horowitz, *Adv. Mater.* **1990**, *2*, 287–292.
- [37] T. J. Marks, *MRS Bull.* **2010**, *35*, 1018.
- [38] F. Diederich, P. J. Stang, R. R. Tykwinski, *Acetylene Chemistry: Chemistry, Biology, and Materials Science*; Wiley-VCH: Weinheim **2005**.
- [39] P.-L. T. Boudreault, J. W. Hennek, S. Loser, R. P. Ortiz, B. J. Eckstein, A. Facchetti, T. J. Marks, *Chem. Mater.* **2012**, *24*, 2929–2942.
- [40] J. Pommerehne, H. Vestweber, W. Guss, R. F. Mahrt, H. Bassler, M. Porsch, J. Daub, *Adv. Mater.* **1995**, *7*, 551–554.
- [41] L. Yang, H. Zhou, W. You, *J. Phys. Chem. C* **2010**, *114*, 16793–16800.
- [42] a) G. Li, V. Shrotriya, J. Huang, Y. Yao, T. Moriarty, K. Emery, Y. Yang, *Nat. Mater.* **2005**, *4*, 864–868; b) X. Guo, M. Zhang, J. Tan, S. Zhang, L. Huo, W. Hu, Y. Li, J. Hou, *Adv. Mater.* **2012**, *24*, 6536–6541; c) X. Guo, M. Zhang, C. Cui, J. Hou, Y. Li, *ACS Appl. Mater. Interfaces* **2014**, *6*, 8190–8198.
- [43] a) G. G. Malliaras, J. R. Salem, P. J. Brock, C. Scott, *Phys. Rev. B* 1998, *58*,

13411–13414; b) V. D. Mihailechi, J. K. J. van Duren, P. W. M. Blom, J. C. Hummelen, R. A. J. Janssen, J. M. Kroon, M. T. Rispens, W. J. H. Verhees, M. M. Wienk, *Adv. Funct. Mater.* **2003**, *13*, 43–46; c) C. Melzer, E. J. Koop, V. D. Mihailechi, P. W. M. Blom, *Adv. Funct. Mater.* **2004**, *14*, 865–870.

Accepted Manuscript

For "Table of Content" only



A new building block ATVTA which uses stiff carbon-carbon triple bonds (A) as the linkages on 1,2-di(2-thienyl)-ethene (TVT) unit has been developed. The effects of the three building blocks (TVT, AT2 and ATVTA units) and the nature of the terminal electron acceptors in some conjugated oligothiophene derivatives were systematically studied.